# Optical and microwave study of a very weak perturbation in high Rydberg states of lutetium

H. Maeda, Y. Matsuo, and M. Takami
*The Institute of Physical and Chemical Research (RIKEN), Wako, Saitama 351-01, Japan*
(Received 28 July 1992)

A very weak perturbation around the $6s^2 52d\ ^2D_{3/2}$ high Rydberg series of Lu has been studied. A line-intensity distribution of the $6s^2nd\ ^2D_{3/2}$ optical transitions exhibits a well-developed Beutler-Fano interference profile with a significant decrease of the radiative lifetime by the configuration interaction. An accurate energy-level structure of the perturbed series is determined by measuring microwave two-photon transitions among the $6s^2nd\ ^2D_{3/2}$ series. The optical line-intensity profiles are analyzed directly by using the eigenfunctions of the perturbed Rydberg series derived from the microwave data. The results are compared with those obtained by the configuration-interaction theory developed by Fano [Phys. Rev. **124**, 1866 (1961)].

PACS number(s): 32.30.Bv, 32.80.Rm, 32.70.Fw, 32.70.Jz

## I. INTRODUCTION

High Rydberg states of neutral many-electron atoms are frequently perturbed by valence states converging to one of the low-lying excited states of ion cores. Such perturbations, which appear locally or in a wide range of series, have been studied extensively in the past two decades by high-resolution laser spectroscopy with the purpose of characterizing the electronic structure of highly excited atoms. In particular, perturbations in Rydberg series of alkaline-earth-metal atoms have attracted many scientists because perturbations in Rydberg series occur frequently by configuration interactions with low-lying doubly excited valence states [1]. The perturbations have been analyzed successfully by the multichannel quantum-defect theory (MQDT) [2], providing detailed knowledge on the electronic level structure and the characteristics of configuration or channel interactions in alkaline-earth-metal atoms.

In contrast to the alkaline-earth-metal atoms, there are very few studies on the Rydberg series of other many-electron atoms such as rare-earth-metal atoms, due primarily to the complexity of their electronic structure. Being motivated by this situation, we started high-resolution laser spectroscopy of the high Rydberg states of Lu. Lutetium is the last member of the 17 rare-earth elements and has a ground-state configuration of $4f^{14}5d6s^2$. Since the $4f$ subshell of Lu is stable below the first ionization limit, the $6s^2nl$ Rydberg series converging to the ground state of Lu II ($4f^{14}6s^2\ ^1S_0$) are hydrogenlike and perturbed with the excited states of the $5d$ electron and/or the $6s$ electron [3]. During the optical survey of the even Rydberg series of Lu [4], we found a very weak and local perturbation in the $6s^2nd\ ^2D_{3/2}$ Rydberg series around $n = 52$ . The perturbation was observed as a prominent intensity dip in the ionization spectrum of the perturbed Rydberg series. Under an electric field over ~50 V/cm, the $J = \frac{3}{2}$ perturbing state was observed clearly as a strong peak in the Stark continuum. Despite the very clear evidence of perturbation, no frequency shifts were observed in nearby lines with the spectral resolution of about 6 GHz. In this experiment, the Rydberg atoms were ionized after a free flight over the distance of several millimeters in length. As a consequence, the delay time between the preparation and the ionization of the Rydberg atoms was not well defined because of the thermal-velocity distribution of the Lu atom.

Recently we reexamined this perturbed Rydberg series with revised experimental techniques in order to study this configuration interaction in detail. Two-step laser photoexcitation spectroscopy with delayed forced ionization was used to study the interference profile, and laser-microwave double-resonance spectroscopy to determine the energy-level structure of the perturbed series with high accuracy. The optical spectrum showed a well-developed Beutler-Fano interference profile over the range of $40 \leq n \leq 60$. Such interference profiles are usually analyzed with the configuration-interaction theory developed by Fano [5]. In the present work, however, the intensity profile was analyzed directly by using the eigenfunctions of a perturbed system calculated during the analysis of the microwave data. The simultaneous analysis of the intensity profile and its delay-time dependence led to an almost complete analysis of the perturbation without ambiguity.

## II. EXPERIMENT

### A. Two-step photoexcitation spectroscopy with delayed forced ionization

High Rydberg Lu atoms were produced between a pair of metal electrodes by irradiating a Lu atomic beam from a resistively heated oven with two pulsed dye-laser beams. The first dye-laser beam at 339.68 nm excited the Lu atoms from the ground state $4f^{14}5d6s^2\ ^2D_{3/2}$ to the intermediate state $4f^{14}6s^27p\ ^2P_{1/2}$ at 29 431.05 $cm^{-1}$ [3]. About 10 ns after the first laser pulse, the second laser excited the atoms further up to one of the Rydberg states that belonged to the $4f^{14}6s^2ns\ ^2S_{1/2}$ or $4f^{14}6s^2nd\ ^2D_{3/2}$ series, either of them being accessible from the interme-

 

diate state by an electric dipole transition. The interaction region was covered with a copper shield which was cooled with liquid nitrogen in order to suppress the effect of blackbody radiation. Two dye lasers were pumped by a XeCl excimer laser. The dye laser had a linear polarization with a maximum output power of a few mJ per pulse and a linewidth of about 6 GHz. Output energy of the first dye laser was attenuated to a few hundred $\mu$J per pulse to avoid ionization of the Lu atom by two-step excitation to the ionization continuum. This laser power was sufficient to saturate the first-step transition. The output energy of the second laser was also attenuated to a similar level in order to avoid saturation of the transitions to the Rydberg states.

After 0.25–1.75 $\mu$s of the second laser pulse, a pulsed voltage of 600 V was applied to the lower electrode for forced ionization of the Rydberg atoms (~600 V/cm). With this electric field we could ionize the Lu Rydberg atoms in the range of $n \geq 34$ for the $6s^2ns\ ^2S_{1/2}$ series and $n \geq 32$ for the $6s^2nd\ ^2D_{3/2}$ series, respectively. Produced ions were then accelerated toward a microchannel plate (MCP) through a grid prepared in the middle of the upper electrode. Finally the ion signals were amplified and averaged with a boxcar integrator, and recorded with a strip chart recorder and simultaneously stored in a personal computer via a computer interface.

### B. Optical-microwave double-resonance spectroscopy

The experimental procedure for the optical-microwave double-resonance spectroscopy is similar to the one used in our previous work on Yb [6]. The Lu atoms in the ground state were excited to one of the $6s^2nd\ ^2D_{3/2}$ Rydberg states as described in Sec. II A. Then the two-photon microwave transition to the $6s^2(n+1)d\ ^2D_{3/2}$ Rydberg state was induced by continuous microwave radiation from one of the several millimeter-wave klystrons, which covered the frequency range of 30–56 GHz and 62–78 GHz. The transition frequency was calibrated with a frequency marker produced by mixing the millimeter wave and higher harmonics of an $X$-band Gunn oscillator, the frequency of which was measured directly with a microwave counter.

Resonance microwave transitions were detected by the selective field-ionization method [7]. After a few $\mu$s from the second laser pulse, a pulsed electric field of appropriate strength (maximum of ~600 V/cm) was applied in order to ionize the atoms in the upper state of the microwave transition selectively. The subsequent procedure for the detection and the recording of ionization spectra was the same as described in Sec. II A.

## III. EXPERIMENTAL RESULTS AND ANALYSIS

### A. Experimental results

#### 1. *Observation of the Beutler-Fano interference in the optical spectra*

Typical Rydberg-series spectra obtained by the two-step photoexcitation and delayed forced-ionization method are shown in Fig. 1 where the delay time between the dye-laser pulse and the pulsed electric field $t_d$ was set to (a) 0.25 $\mu$s, (b) 0.75 $\mu$s, and (c) 1.75 $\mu$s, respectively. These spectra include the $6s^2ns\ ^2S_{1/2}$ series for $42 \leq n \leq 62$ and the $6s^2nd\ ^2D_{3/2}$ series for $40 \leq n \leq 60$. The term values of these series have already been measured in our previous study of the Lu Rydberg series [4]. One can clearly recognize the asymmetric line-intensity distribution in the $6s^2nd\ ^2D_{3/2}$ series spectra reflecting the Beutler-Fano interference effect.

Another important feature in the optical spectra is the rapid change of the line-intensity profile as $t_d$ changes from 0.25 to 1.75 $\mu$s. The asymmetry of the line-intensity profile becomes inconspicuous as $t_d$ increases. (This is the reason why we failed to observe the Beutler-Fano inter-

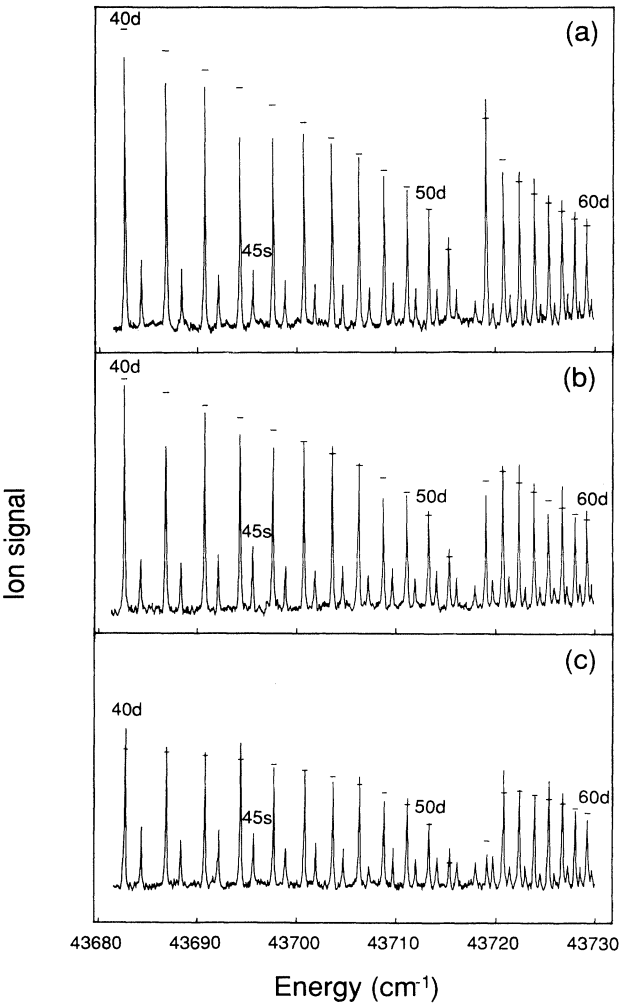


FIG. 1. Typical traces of two-step photoexcitation spectra with delayed forced ionization. The $6s^2ns\ ^2S_{1/2}$ and $6s^2nd\ ^2D_{3/2}$ series are excited and ionized via the $6s^27p\ ^2P_{1/2}$ intermediate state. Delay time between the laser and the pulsed electric field $t_d$ is (a) 0.25 $\mu$s, (b) 0.75 $\mu$s, and (c) 1.75 $\mu$s, respectively. The calculated intensities of the $6s^2nd\ ^2D_{3/2}$ series by Eq. (16) with the parameters listed in Table IV are shown as short bars.

ference profile in our previous experiment in which the average delay time was several $\mu$s.) This implies that the radiative decay rate of the Rydberg states dramatically increases around $n = 52$ due to the admixture of the valence-state character. This strong delay-time dependence of the line intensity is due to a very short radiative lifetime of the perturber, 8(1) ns, which was determined by deconvolution of the fluorescence-decay curve. Thus the radiative lifetime of the Rydberg state is highly sensitive to a very weak perturbation.

#### *2. Measurement of the microwave-transition frequencies*

We measured the energy differences between the neighboring Rydberg states by optical-microwave double resonance to determine the energy-level structure of the perturbed series accurately. The measured microwave transitions were the $6s^2(n+1)d\ ^2D_{3/2} \leftarrow\leftarrow 6s^2nd\ ^2D_{3/2}$ two-photon transitions in the range of $38 \leq n \leq 49$. This assignment was based on the transition frequencies predicted by the Rydberg-Ritz formula [see Eq. (2)] using the quantum defects given in Ref. [4]. The transitions near the perturber could not be measured because of the short radiative lifetimes of the perturbed Rydberg states. Figure 2 shows a typical trace of the microwave-transition line. The linewidth of the microwave transitions, usually in the order of MHz [full width at half maximum (FWHM)], has been limited mainly by the frequency instability of the klystron. Hyperfine structures in the Rydberg states could not be resolved in this experiment although $^{175}$Lu has an extremely large nuclear quadrupole moment [8]. All the measured frequencies are given in the second column of Table I.

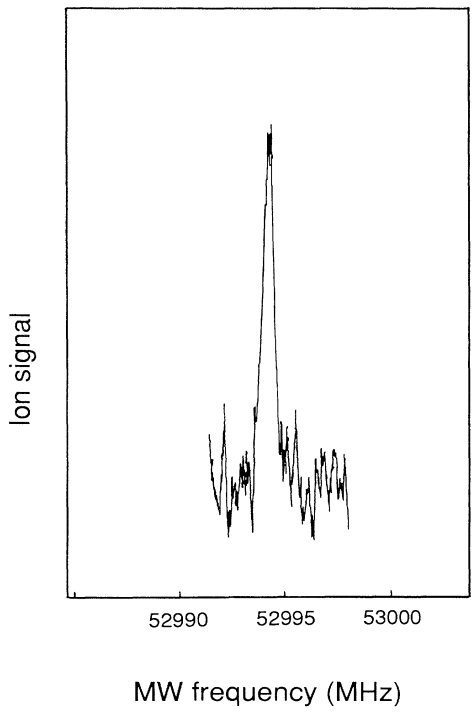


FIG. 2. A typical spectral profile of the $6s^247d\ ^2D_{3/2} \leftarrow\leftarrow 6s^246d\ ^2D_{3/2}$ microwave two-photon transition.

TABLE I. The $6s^2(n+1)d\ ^2D_{3/2} \leftarrow\leftarrow 6s^2nd\ ^2D_{3/2}$ transitions. The energy interval of this transition corresponds to twice the measured frequency.

| $n$ | Observed frequency (MHz) | Calculated frequency (MHz) | Observed minus calculated (MHz) |
|---|---|---|---|
| 38 | 72908.91 | 72908.83 | 0.08 |
| 39 | 67103.34 | 67103.43 | -0.09 |
| 40 | | 61897.68 | |
| 41 | | 57216.17 | |
| 42 | 52994.54 | 52994.59 | -0.05 |
| 43 | 49177.78 | 49177.83 | -0.05 |
| 44 | 45718.46 | 45718.49 | -0.03 |
| 45 | 42575.76 | 42575.61 | 0.15 |
| 46 | 39713.66 | 39713.63 | 0.03 |
| 47 | 37101.44 | 37101.42 | 0.02 |
| 48 | 34711.16 | 34711.25 | -0.09 |
| 49 | 32516.54 | 32516.52 | 0.02 |

### B. Analysis of the experimental data

In the present work, exceptionally rich spectroscopic data have been obtained for the weak perturbation in the $6s^2nd\ ^2D_{3/2}$ series. A proper approach to analyze the observed optical line-intensity profile and its delay-time dependence should include the Beutler-Fano interference effect and the enhancement of the radiative decay rate of the perturbed Rydberg states simultaneously. Such an approach has already been discussed in the early work of Sandner, Safinya, and Gallagher to predict the line-intensity profile of a perturbed Rydberg series [9]. In the present work, however, the observed intensity profiles were analyzed directly by using the eigenfunctions of the perturbed Rydberg states obtained by the analysis of microwave data. In the following section, we briefly introduce the theoretical background necessary for the present analysis and the conventional configuration-interaction theory for comparison with our method of analysis.

#### *1. Theoretical background*

Matrix elements of a Hamiltonian of an atomic system constructed with one Rydberg series and one perturbing valence state are given by [5]

$$\langle \varphi \mid H \mid \varphi \rangle = E_\varphi \,, \tag{1a}$$

$$\langle \psi_n \mid H \mid \varphi \rangle = V_n \,, \tag{1b}$$

$$\langle \psi_m \mid H \mid \psi_n \rangle = E_n \delta_{mn} \,, \tag{1c}$$

where $\varphi$ and $\psi_n$ denote a valence state of energy $E_\varphi$ and an unperturbed pure Rydberg state of energy $E_n$ with the principal quantum number $n$. Square of the off-diagonal matrix element $V_n$ gives an index of the strength of configuration interaction. The energy $E_n$ of the pure Rydberg state is represented by the general Rydberg-Ritz formula,

$$E_n = -\frac{R}{(n-\delta_n)^2}\,, \tag{2}$$

where $R$ is the Rydberg constant for a corresponding atom and $\delta_n$ is the quantum defect of the form [10],

$$\delta_n = \delta_0 + \frac{\delta_1}{(n-\delta_n)^2} + \cdots\,. \tag{3}$$

The eigenfunction of this system can be written as a linear combination of $\varphi$ and $\psi_n$,

$$\Psi_\nu = a_\nu \varphi + \sum_j b_\nu(j)\psi_j\,, \tag{4}$$

where the subscript $\nu$ labels both the perturbed valence state [$\nu = \nu(\varphi)$] and the perturbed Rydberg states [$\nu = \nu(n)$] simultaneously, i.e., $\{\nu\} = \{n, \varphi\}$. Squares of the coefficients $a_\nu$ and $b_\nu(j)$ are determined by the ordinary perturbation theory and the orthonormalization condition for the eigenfunction $\Psi_\nu$. When the condition $|\,V_n\,| \ll |\,E_n - E_\varphi\,|$ is satisfied, the energy of the perturbed Rydberg state is given by

$$\begin{aligned}\tilde{E}_n &\equiv E_{\nu(n)} \quad (\nu \neq \varphi) \\ &= E_n + \Delta E_n \\ &= -\frac{R}{(n-\delta_n)^2} + \frac{|\,V_n\,|^2}{E_n - E_\varphi}\,.\end{aligned} \tag{5}$$

Hereafter we use a tilde to denote the perturbed parameters when the subscript $\nu$ does not need to cover $n$ and $\varphi$ simultaneously.

Since the configuration interaction is regarded as a core effect, one can relate the square of the off-diagonal matrix element (1b) to the normalized coupling constant $V$ as

$$|\,V_n\,|^2 \simeq \frac{V^2}{n^{*3}}, \tag{6}$$

where $n^*$ $(= n - \delta_n)$ is an effective quantum number, and $V$ is assumed to be constant over the range of $n$ studied in the present work. Note that the change in the quantum defect due to the perturbation of the valence state becomes, to a good approximation,

$$\tilde{\delta}_n = \delta_n - \frac{V^2/(2R)}{E_n - E_\varphi}, \tag{7}$$

when $|\,E_n\,| \gg |\,\Delta E_n\,|$ is satisfied [11]. This leads to Langer's formula [12] by replacing $\delta_n$ in Eq. (2) with the above $\tilde{\delta}_n$.

In Fano's theory, the relative change of the electric dipole-transition probability by a perturbation, i.e., the transition probability from a low-lying state $i$ to the perturbed continuum state $\tilde{\psi}_E$ divided by the one from $i$ to the unperturbed continuum state $\psi_E$, is given in terms of two parameters $q$ and $\varepsilon$ by

$$\frac{|\langle\tilde{\psi}_E \mid r \mid i\rangle|^2}{|\langle\psi_E \mid r \mid i\rangle|^2} = \frac{(q+\varepsilon)^2}{1+\varepsilon^2}\,. \tag{8}$$

Here the parameter $q$ is defined by

$$q = \frac{\langle\Phi \mid r \mid i\rangle}{\pi V_E \langle\psi_E \mid r \mid i\rangle}, \tag{9}$$

where $\Phi$ is the eigenfunction of the discrete valence state modified by an admixture of the continuum state and $V_E$ is the configuration-interaction matrix element between the discrete and continuum state at energy $E$. The reduced energy variable $\varepsilon$ is given by

$$\varepsilon = \frac{E - E_\varphi - F}{\pi\,|\,V_E\,|^2}, \tag{10}$$

where $F$ is a function of the energy [see Eq. (8) of Ref. [5]].

Equation (8) represents the effect of the phase interference on the spectral profile of the autoionizing state. The same formalism is applicable to represent the ratio of the transition probability from a low-lying state $i$ to a perturbed Rydberg state $\tilde{\psi}_n$ and from $i$ to that of the pure Rydberg state $\psi_n$ as will be discussed later. It should be noted that when applying Eq. (8) to the evaluation of the transition probability from a low-lying state to a perturbed Rydberg state, care must be taken in the difference between the normalization condition for the continuum wave functions and that for the bound-state wave functions.

### 2. *Analysis of the microwave-transition data*

The energy differences between the nearby $6s^2nd\ ^2D_{3/2}$ Rydberg states measured by microwave spectroscopy were first analyzed in order to determine the spectroscopic parameters $E_n$ (i.e., $\delta_0, \delta_1, \ldots$), $E_\varphi$, $V_n$ (or $V$), and the mixing coefficients $\tilde{a}_n$ and $\tilde{b}_n$ [see Eqs. (1)–(4)]. For this purpose, the energy matrix, which contains $E_n$ and $E_\varphi$ as diagonal terms and $V_n = V/(n^*)^{3/2}$ as off-diagonal terms, was directly diagonalized to calculate the eigenvalues $\tilde{E}_n$ and $\tilde{E}_\varphi$. The parameters were determined by a least-squares fit of these eigenvalues to the measured energy separations,

$$\Delta E[6s^2(n+1)d \longleftarrow\!\!\!\!\!\!\leftarrow 6s^2nd] = \tfrac{1}{2}[\tilde{E}_{n+1} - \tilde{E}_n]\,. \tag{11}$$

Note that we have dealt with the quantum defect $\delta_n$ as

$$\delta_n = \delta_0 + \frac{\delta_1}{(n-\delta_0)^2} + \cdots\,, \tag{3'}$$

for the sake of simplifying the numerical computation. The final fitting parameters are listed in Table II. The calculated transition frequencies are listed in the third column of Table I with the differences between the observed and calculated frequencies in the forth column, which are mostly less than 100 kHz. The squares of the

TABLE II. Spectroscopic parameters for the $6s^2nd\ ^2D_{3/2}$ Rydberg series of Lu determined from the microwave data. Numbers in parentheses are one standard deviations in units of the last significant digits.

| $\delta_0$ | $\delta_1$ | $V$(GHz) | $E_\varphi$ (GHz) |
|---|---|---|---|
| 2.92659(9) | -24.56(7) | $1.23(2)\times10^3$ | -1358(3) |

TABLE III. The mixing coefficient $|a_\nu|^2$ and $|b_\nu(n)|^2$. A blank space corresponds to zero.

| $\nu$ | ... | $\lvert b_\nu(50)\rvert^2$ | $\lvert b_\nu(51)\rvert^2$ | $\lvert b_\nu(52)\rvert^2$ | $\lvert a_\nu\rvert^2$ | $\lvert b_\nu(53)\rvert^2$ | $\lvert b_\nu(54)\rvert^2$ | ... |
|---|---|---|---|---|---|---|---|---|
| ⋮ | | | | | ⋮ | | | |
| 50 | | 0.9991 | | | 0.0009 | | | |
| 51 | | | 0.9968 | | 0.0032 | | | |
| 52 | ... | 0.0001 | 0.0006 | 0.8682 | 0.1302 | 0.0005 | 0.0001 | ... |
| $\varphi$ | ... | 0.0008 | 0.0026 | 0.1318 | 0.8564 | 0.0051 | 0.0011 | ... |
| 53 | | | | | 0.0056 | 0.9943[a] | | |
| 54 | | | | | 0.0012 | | 0.9988 | |
| ⋮ | | | | | ⋮ | | | |

[a]This value contains a round-off error.

mixing coefficients, $|a_\nu|^2$ and $|b_\nu|^2$, are listed in Table III.

It should be noted that the interaction energy, $V_n = V/(n^*)^{3/2}$, is approximately 0.12 $cm^{-1}$ at $n = 52$, which is much weaker compared with the perturbations in the high Rydberg series reported so far [13]. The maximum energy shift among the observed optical transitions is 260 MHz for $n = 53$, which is much less than the 6-GHz spectral resolution with our pulsed dye laser. This was the reason why we failed to observe the energy shift of the perturbed Rydberg series in the optical spectra. The weakness of the perturbation is also observed as a very localized mixing of the perturber in the eigenfunctions of the Rydberg states as shown in Table III.

### 3. *Analysis of the line-intensity distribution of the optical spectra*

Next we analyze the intensity profile of the optical spectra shown in Fig. 1. Under the assumption that the ionization probabilities of all the Rydberg states are the same, the intensity profile of the optical spectra depends on the transition probability and the radiative decay rate of each state as stated in Sec. III A 1. The transition probability from a low-lying state to a perturbed Rydberg series is usually expressed in terms of Fano's $q$ and $\varepsilon$ parameters according to the conventional configuration-interaction theory [see Eq. (8)]. However, we calculated the transition probability directly by using the eigenfunctions of the perturbed Rydberg states derived from the analysis of the microwave data. With this method, reliable analysis of the intensity profile was achieved which led to the determination of the ratio of the transition probabilities as well as the decay rate of the perturbed system in the following manner.

From Eq. (4), we can write the electric dipole-transition probability from a low-lying state $i$ to the $n$th perturbed Rydberg state as

$$\begin{aligned}\tilde{I}_n^{pe} &= A'|\langle\tilde{\psi}_n \mid r \mid i\rangle|^2 \\ &= A'\left|\tilde{a}_n\langle\varphi \mid r \mid i\rangle + \sum_j \tilde{b}_n(j)\langle\psi_j \mid r \mid i\rangle\right|^2 \\ &= A\left|\tilde{a}_n\bar{q} + \sum_j \tilde{b}_n(j)/(j^*)^{3/2}\right|^2 , \end{aligned} \tag{12}$$

where $\tilde{I}_n^{pe}$ is the perturbed transition probability, $A$ [$= A'(n^*)^3|\langle\psi_n \mid r \mid i\rangle|^2$] is a scaling factor to the experimental values, and a parameter $\bar{q}$ is defined by

$$\bar{q} = \frac{\langle\varphi \mid r \mid i\rangle}{(n^*)^{3/2}\langle\psi_n \mid r \mid i\rangle} . \tag{13}$$

Here the parameter $\bar{q}$ has a simple physical meaning that it is the ratio of the transition-matrix element to the perturber, $\langle\varphi \mid r \mid i\rangle$, and the normalized transition-matrix element to the unperturbed Rydberg state, $(n^*)^{3/2}\langle\psi_n \mid r \mid i\rangle$. The $A$ and $\bar{q}$ parameters, between which only $\bar{q}$ is physically meaningful, are assumed to be independent of $n^*$ as assumed for the normalized coupling constant $V$ in Eq. (6). Thus the transition probability $\tilde{I}_n^{pe}$ is determined by the coefficients $\tilde{a}_n$ and $\tilde{b}_n$ derived from the microwave data, and the two adjustable parameters, $A$ and $\bar{q}$.

As mentioned previously, the intensity of the optical spectrum also depends on the delay time $t_d$ between the excitation laser pulse and the ionization-field pulse. The radiative decay rates of the Rydberg states with low angular momentum also have the $(n^*)^{-3}$ dependence, so that the decay rate for the $n$th perturbed Rydberg state $\tilde{\Gamma}_n$ is evaluated with a simple form,

$$\tilde{\Gamma}_n \simeq |\tilde{a}_n|^2\gamma_\varphi + \sum_j |\tilde{b}_n(j)|^2\gamma_{\mathrm{Ryd}}/(j^*)^3 , \tag{14}$$

where $\gamma_\varphi$ and $\gamma_{\mathrm{Ryd}}/(j^*)^3$ represent the decay rates of the valence state and the $j$th pure Rydberg state, respectively [14, 15]. Thus the influence of the decay time on the intensity of the optical spectrum is expressed by a factor of

$$\tilde{I}_n^{rd}(t) = \exp(-\tilde{\Gamma}_n t) . \tag{15}$$

Consequently, the relative line intensity of the optical spectra of the $n$th perturbed Rydberg state is given by

$$\begin{aligned}\tilde{I}_n(t) &= \tilde{I}_n^{pe}\tilde{I}_n^{rd}(t) \\ &= A\left|\tilde{a}_n\bar{q} + \sum_j \tilde{b}_n(j)/(j^*)^{3/2}\right|^2 \exp(-\tilde{\Gamma}_n t) . \end{aligned} \tag{16}$$

The observed optical spectra were fitted to the above expression with $A$, $\bar{q}$, $\gamma_\varphi$, and $\gamma_{\mathrm{Ryd}}$ as adjustable param-

TABLE IV. Parameters determined by fitting the experimental data to Eq. (16). Numbers in parentheses are one standard deviations in units of the last significant digits.

| $\bar{q}$ | $\gamma_\varphi$ ($s^{-1}$) | $\gamma_{\rm Ryd}$ ($s^{-1}$) |
|---|---|---|
| 0.0137(7) | $1.3(1)\times10^8$ | $2.5(2)\times10^{10}$ |

eters. This fitting was performed with all the Rydberg data throughout the region of $40 \le n \le 60$ for the delay time $t_d$ = 0.25, 0.75, and 1.75 $\mu$s. The calculated line intensities are represented in Fig. 1 as short bars. The agreement between the observed and the calculated line intensities is satisfactory. The final fitting parameters are listed in Table IV.

## IV. DISCUSSION

In the above analysis, we introduced a parameter $\bar{q}$ for the direct analysis of observed intensity profiles by using the eigenfunctions of the perturbed Rydberg states. Here we relate the $\bar{q}$ parameter with Fano's $q$ parameter first. From the definition of the $q$ parameter in Eq. (9), one can derive the following expression from Eq. (23) and subsequent discussion in Ref. [5],

$$q^2 - 1 = \frac{|\langle\varphi \mid r \mid i\rangle|^2}{\pi^2 |V_E|^2 |\langle\psi_E \mid r \mid i\rangle|^2}. \tag{17}$$

Since this expression is derived for the case of a continuum state perturbed with a valence state, we have to transform the above expression to the case of perturbed Rydberg states by introducing the parameter, $\tau_n \approx 2R/(n^*)^3$, which is the average of the nearest two-level spacings (see Appendix B of Ref. [5]). By substituting $|V_E|^2 = |V_n|^2/\tau_n$ and $|\langle\psi_E \mid r \mid i\rangle|^2 = |\langle\psi_n \mid r \mid i\rangle|^2/\tau_n$, one can finally obtain the relation

$$\begin{aligned} q^2 - 1 &= \frac{4R^2 |\langle\varphi \mid r \mid i\rangle|^2}{\pi^2 V^2 (n^*)^3 |\langle\psi_n \mid r \mid i\rangle|^2} \\ &= \frac{4R^2}{\pi^2 V^2} \bar{q}^2 . \end{aligned} \tag{18}$$

In order to find the consistency of our analysis with the one based on the configuration-interaction theory, we determined the $q$ value by fitting the following equation to the optical spectra in Fig. 1:

$$\tilde{I}_n(t) = \frac{A''}{(n^*)^3} \frac{(q+\varepsilon_n)^2}{1+\varepsilon_n{}^2} \exp(-\tilde{\Gamma}_n t), \tag{19}$$

where $A''$ is a scaling factor, and the factor $(n^*)^3$ in the denominator arises from the denominator on the left-hand side of Eq. (8), i.e., the $(n^*)^{-3}$ dependence of $|\langle\psi_n \mid r \mid i\rangle|^2$. The third factor is equal to Eq. (15). For the quantity $\varepsilon_n$, we used the following approximated expression:

$$\varepsilon_n \simeq \frac{\tilde{E}_n - \tilde{E}_\varphi}{\pi |V_n|^2 / \tau_n}. \tag{10'}$$

The best fit was attained with the value of $q$ = 23(1). This is almost in exact agreement with the value $q$ = 23.2 calculated from $\bar{q}$ using Eq. (18).

The parameters $\gamma_\varphi$ and $\gamma_{\rm Ryd}$ represent the decay rates of the pure valence state and the normalized decay rate of the Rydberg state. Knowing the value of $\gamma_\varphi$, we extracted from Eq. (14) the lifetime of the modified valence state to be 8.9 ns. This value is within the error limit of the experimental value, 8(1) ns. The normalized decay rate of the Rydberg state, $\gamma_{\rm Ryd} = 2.5\times10^{10}$ $s^{-1}$, seems to be in a reasonable range because the experimental value for the $6snd\ ^1D_2$ Rydberg state of Ba is $\gamma_1 = 5.9\times10^9$ $s^{-1}$ [15], and the calculated value for the $D$ state of Cs is $1.0\times10^9$ $s^{-1}$ [16]. However, our value should be regarded as an upper limit because both the redistribution of the Rydberg states by a blackbody radiation and the collisional quenching of the Rydberg states increase the decay rate, particularly in the region of high principal quantum number $n$ as studied in the present work. In our experiment, the temperature of the resistively heated oven is about 1600 K to evaporate Lu which has a melting point of 1925 K. We made a rough estimate of the influence of the blackbody radiation at this temperature to the decay rate by the procedure of Cooke and Gallagher [17]. However, the estimated increase of the decay rate at the interaction region, which was about 30 cm off the oven, was 1.7–0.7 $\times$ $10^4$ $s^{-1}$ for $n$ = 40 − 60 and negligible compared to the measured value.

Weak perturbations in high Rydberg states have been studied in the Ba $6sng\ ^1G_4$ series around $n$ = 24 by Gallagher *et al.* [13] and in the Ba $6snd\ ^1D_2$ series around $n$ = 26 by Sandner, Safinya, and Gallagher [9]. In the present work, however, the perturbation was observed under the circumstances much more favorable for the extensive spectroscopic study. First, the perturbation was observed in the region of large principal quantum number. The high spectral density in such a region allowed us to measure the $n$ dependence of the optical transition intensity over the wide range of $n$. Furthermore, the level spacing in this region was in the proper range to be measured with microwave two-photon transitions. The accurate microwave data were essential to determine the $n$-dependent character of the present configuration interaction. The second is the short radiative lifetime of the perturber, which is about $\frac{1}{20}$ of the one observed in the $6sng\ ^1G_4$ high Rydberg series of Ba [13]. This short radiative lifetime allowed us to detect a very weak perturbation clearly as the delay-time dependence of the optical transition intensities. Actually, the normalized coupling energy in the present series is 25 times smaller than the one observed in the $6sng\ ^1G_4$ high Rydberg series of Ba. The actual coupling energy in Lu is further reduced by one order of magnitude by a larger number of $n$ for the perturbed state.

In the present work, the observed Fano interference profile was analyzed by using the eigenfunctions of the perturbed Rydberg states determined by the analysis of microwave data. This method has an advantage that the analysis is straightforward because the phase shifts of the perturbed wave functions, which are the origin of the interference profile, are introduced automatically during the diagonalization process of the energy matrix.

Also, the parameter $\bar{q}$ introduced in the present work has a much clearer physical meaning than Fano's $q$ parameter, at least for the case of the perturbed Rydberg series. However, a good agreement of the $q$ parameters derived by these two methods implies that when the perturbation is weak, both treatments are equally satisfactory. One problem in applying Fano's theory to a perturbed Rydberg series is that one has to use approximations for transforming the theory, which was developed originally for the case of perturbed continuum states, to the case of perturbed discrete states. From this point of view, an interesting case for testing the validity of the present treatment will be a strongly perturbed high Rydberg series, for which perturbation theory is not applicable. Although the present method has limited applicability, it will be worth extending this method to the analysis of other perturbed systems.

[1] See, for example, J.A. Armstrong, J.J. Wynne, and P. Esherick, J. Opt. Soc. Am. **69**, 211 (1979).
[2] M.J. Seaton, Rep. Prog. Phys. **46**, 167 (1983).
[3] W.C. Martin, R. Zalubas, and L. Hagan, *Atomic Energy Levels. The Rare-Earth Elements*, Natl. Bur. Stand. Ref. Data Ser., Natl. Bur. Stand. (U.S.) Circ. No. 60 (U.S. GPO, Washington, D.C., 1978).
[4] H. Maeda, Y. Mizugai, Y. Matsumoto, A. Suzuki, and M. Takami, J. Phys. B **22**, L511 (1989).
[5] U. Fano, Phys. Rev. **124**, 1866 (1961).
[6] H. Maeda, Y. Matsuo, M. Takami, and A. Suzuki, Phys. Rev. A **45**, 1732 (1992).
[7] T.W. Ducas, M.G. Littman, R.R. Freeman, and D. Kleppner, Phys. Rev. Lett. **35**, 366 (1975).
[8] H. Kopfermann, *Nuclear Moments* (Academic, New York, 1958).
[9] W. Sandner, K.A. Safinya, and T.F. Gallagher, Phys. Rev. A **33**, 1008 (1986).
[10] B. Edlén, *Encyclopedia of Physics* (Springer, Berlin, 1964), Vol. 27, p. 123.
[11] W.R.S. Garton, J. Quant. Spectrosc. Radiat. Transfer. **2**, 335 (1962).
[12] R.M. Langer, Phys. Rev. **35**, 649 (1930).
[13] T.F. Gallagher, F. Gounand, R. Kachru, N.H. Tran, and P. Pillet, Phys. Rev. A **27**, 2485 (1983).
[14] T.F. Gallagher, W. Sandner, and K.A. Safinya, Phys. Rev. A **23**, 2969 (1981).
[15] M. Aymar, R-J. Champeau, C. Delsart, and J-C. Keller, J. Phys. B **14**, 4489 (1981).
[16] F. Gounand, J. Phys. (Paris) **40**, 457 (1979).
[17] W.E. Cooke and T.F. Gallagher, Phys. Rev. A **21**, 588 (1980).